

# Search for anomalous quartic $WWZ\gamma$ couplings at the future linear $e^+e^-$ collider

M. Köksal\*

*Department of Physics, Cumhuriyet University, 58140, Sivas, Turkey*

A. Senol†

*Department of Physics, Kastamonu University,  
37100, Kuzeykent, Kastamonu, Turkey*

## Abstract

In this work, the potential of two different processes  $e^+e^- \rightarrow W^-W^+\gamma$  and  $e^+e^- \rightarrow e^+\gamma^*e^- \rightarrow e^+W^-Z\nu_e$  at the Compact Linear Collider (CLIC) to probe the anomalous quartic  $WWZ\gamma$  gauge couplings is examined. For  $\sqrt{s} = 0.5, 1.5$  and 3 TeV energies of the CLIC, we find 95% confidence level limits on the anomalous coupling parameters defining the dimension-six operators in a model independent way by means of the effective Lagrangian approach. We show that the best limits obtained on the anomalous couplings  $\frac{k_0}{\Lambda^2}$ ,  $\frac{k_c}{\Lambda^2}$  and  $\frac{a_n}{\Lambda^2}$  for the integrated luminosity of  $L_{int} = 590$  fb $^{-1}$  at the CLIC with  $\sqrt{s} = 3$  TeV are  $[-1.75; 1.50] \times 10^{-6}$  GeV $^{-2}$ ,  $[-3.21; 2.47] \times 10^{-6}$  GeV $^{-2}$  and  $[-9.13; 9.09] \times 10^{-7}$  GeV $^{-2}$ , respectively.

---

\*mkoksal@cumhuriyet.edu.tr

†asenol@kastamonu.edu.tr

## I. INTRODUCTION

The Standard Model (SM) of particle physics has been demonstrated to be quite successful until now through very important experimental tests, particularly after the recent discovery of the new particle with a mass of about 125 GeV which is consistent with the SM Higgs boson [1, 2]. However, the SM does not answer some of the most fundamental questions such as the origin of mass, the large hierarchy between electroweak and Planck scale, the strong CP problem, and matter - antimatter asymmetry. To clarify these questions, new physics beyond the SM is needed. A simple way to discover new physics beyond SM is to probe anomalous gauge boson self interactions. In the electroweak sector of SM, gauge boson self interactions are completely determined by  $SU_L(2) \times U_Y(1)$  gauge invariance. Hence, the high precision measurements of gauge boson self interactions are extremely important in the understanding of the gauge structure of the SM. Any deviation from the expected values of these couplings would imply the existence of new physics beyond the SM. Investigation of the new physics through effective Lagrangian method is a well known approach. The origin of this method is based on the assumption that at high energies above the SM, there is a grander theory which reduces to the SM at lower energies. Therefore, SM is supposed to be an effective low energy theory in which heavy fields have been integrated out. Since this fundamental method is independent of the details of the model, it is occasionally called model independent analysis.

In this paper, we examine the anomalous quartic  $WWZ\gamma$  gauge boson couplings by analyzing the two different processes  $e^+e^- \rightarrow W^-W^+\gamma$  and  $e^+e^- \rightarrow e^+\gamma^*e^- \rightarrow e^+W^-Z\nu_e$  at the CLIC. Genuine quartic couplings consisting of effective operators, have different origins than anomalous trilinear gauge boson couplings. Hence, we assume that genuine quartic gauge couplings can be independently analysed from the effects arising from any trilinear gauge couplings. In the literature, to examine the genuine quartic  $WWZ\gamma$  couplings, there are usually two different dimension 6 effective quartic Lagrangians that keep custodial  $SU(2)_c$  symmetry and local  $U(1)_{QED}$  symmetry. The first one, CP-violating effective Lagrangian is given as the following [3]

$$L_n = \frac{i\pi\alpha}{4\Lambda^2} a_n \epsilon_{ijk} W_{\mu\alpha}^{(i)} W_{\nu}^{(j)} W^{(k)\alpha} F^{\mu\nu} \quad (1)$$

where  $\alpha$  is the electroweak coupling constant,  $W^{(i)}$  is the  $SU(2)_c$  weak isospin triplet,  $F_{\mu\nu} =$

$\partial_\mu A_\nu - \partial_\nu A_\mu$  is the tensor for electromagnetic field strength,  $a_n$  represents the strength of anomalous coupling and  $\Lambda$  represents the energy scale of possible new physics. The anomalous vertex for  $W^+(p_+^\mu)W^-(p_-^\nu)Z(p_1^\alpha)\gamma(p_2^\beta)$  with the help of effective Lagrangian (1) is generated as follows

$$\begin{aligned}
& i \frac{\pi\alpha}{4\cos\theta_W\Lambda^2} a_n [g_{\mu\alpha}[g_{\nu\beta}p_2\cdot(p_1 - p_+) - p_{2\nu}\cdot(p_1 - p_+)\beta] \\
& - g_{\nu\alpha}[g_{\mu\beta}p_2\cdot(p_1 - p_-) - p_{2\mu}\cdot(p_1 - p_-)\beta] \\
& + g_{\mu\nu}[g_{\alpha\beta}p_2\cdot(p_+ - p_-) - p_{2\alpha}\cdot(p_+ - p_-)\beta] \\
& - p_{1\mu}(g_{\nu\beta}p_{2\alpha} - g_{\alpha\beta}p_{2\nu}) + p_{1\nu}(g_{\mu\beta}p_{2\alpha} - g_{\alpha\beta}p_{2\mu}) \\
& - p_{-\alpha}(g_{\mu\beta}p_{2\nu} - g_{\nu\beta}p_{2\mu}) + p_{+\alpha}(g_{\nu\beta}p_{2\mu} - g_{\mu\beta}p_{2\nu}) \\
& + p_{+\nu}(g_{\alpha\beta}p_{2\mu} - g_{\mu\beta}p_{2\alpha}) + p_{-\mu}(g_{\alpha\beta}p_{2\nu} - g_{\nu\beta}p_{2\alpha})].
\end{aligned} \tag{2}$$

Second, CP-conserving effective Lagrangian can be given by [4]

$$L = L_0 + L_c \tag{3}$$

$$L_0 = -e^2 g^2 \frac{k_0}{\Lambda^2} F_{\mu\nu} Z^{\mu\nu} W^{+\alpha} W_\alpha^-, \tag{4}$$

$$L_c = -\frac{e^2 g^2}{2} \frac{k_c}{\Lambda^2} F_{\mu\nu} Z^{\mu\alpha} (W^{+\nu} W_\alpha^- + W^{-\nu} W_\alpha^+) \tag{5}$$

where  $g = e/\sin\theta_W$ ,  $k_0$  and  $k_c$  are the dimensionless anomalous coupling constants. The vertex functions for  $W^+(p_1^\alpha)W^-(p_2^\beta)Z(k_2^\nu)\gamma(k_1^\mu)$  produced from the effective Lagrangians (4) and (5) are expressed respectively by

$$i \frac{e^2 g^2}{\Lambda^2} 2k_0 g_{\alpha\beta} [g_{\mu\nu}(k_1\cdot k_2) - k_{1\nu}k_{2\mu}], \tag{6}$$

$$\begin{aligned}
& i \frac{e^2 g^2}{2\Lambda^2} k_c [(g_{\mu\alpha}g_{\nu\beta} + g_{\nu\alpha}g_{\mu\beta})(k_1\cdot k_2) + g_{\mu\nu}(k_{2\beta}k_{1\alpha} + k_{1\beta}k_{2\alpha}) \\
& - k_{2\mu}k_{1\alpha}g_{\nu\beta} - k_{2\beta}k_{1\nu}g_{\mu\alpha} - k_{2\alpha}k_{1\nu}g_{\mu\beta} - k_{2\mu}k_{1\beta}g_{\nu\alpha}].
\end{aligned} \tag{7}$$

Anomalous quartic  $WWZ\gamma$  couplings at linear colliders and their  $e\gamma$  and  $\gamma\gamma$  modes have been examined through the processes  $e^+e^- \rightarrow W^+W^-Z, W^+W^-\gamma, W^+W^-(\gamma) \rightarrow 4f\gamma$  [5–10],  $e\gamma \rightarrow W^+W^-e, \nu_e W^-Z$  [3, 11] and  $\gamma\gamma \rightarrow W^+W^-Z$  [12, 13]. These couplings appear as  $eW^-W^+$  and  $\nu_e ZW^-$  final state productions of  $e\gamma$  collision of linear colliders.  $\nu_e ZW^-$  production is more sensitive to anomalous quartic  $WWZ\gamma$  couplings with respect to  $eW^-W^+$  production [3]. This production isolates the anomalous  $WWZ\gamma$  couplings from  $WW\gamma\gamma$  couplings. These couplings have also been investigated at the Large Hadron Collider (LHC) via the processes  $pp \rightarrow W(\rightarrow jj)\gamma Z(\rightarrow \ell^+\ell^-)$  [14] and  $pp \rightarrow W(\rightarrow \ell\nu_\ell)\gamma Z(\rightarrow \ell^+\ell^-)$  [15]. Although anomalous quartic  $WWZ\gamma$  couplings have been examined in many studies by analyzing either CP-violating or CP-conserving effective Lagrangians in the literature, these couplings have been investigated using two effective Lagrangians only by Ref. [15].

On the other hand, the limits on  $a_n/\Lambda^2$  parameter of the anomalous quartic  $WWZ\gamma$  couplings are constrained at the LEP by analysing the process  $e^+e^- \rightarrow W^+W^-\gamma$  [16–18]. This reaction is sensitive to both the anomalous  $WW\gamma\gamma$  and  $WWZ\gamma$  couplings.

The latest results obtained by L3, OPAL and DELPHI collaborations are given by  $-0.14 \text{ GeV}^{-2} < \frac{a_n}{\Lambda^2} < 0.13 \text{ GeV}^{-2}$ ,  $-0.16 \text{ GeV}^{-2} < \frac{a_n}{\Lambda^2} < 0.15 \text{ GeV}^{-2}$ , and  $-0.18 \text{ GeV}^{-2} < \frac{a_n}{\Lambda^2} < 0.14 \text{ GeV}^{-2}$  at 95% confidence level (C. L.), respectively. However, the recent most restrictive experimental limits on  $k_0/\Lambda^2$  and  $k_c/\Lambda^2$  parameters of the anomalous quartic  $WWZ\gamma$  couplings are determined through the process  $q\bar{q}' \rightarrow W(\rightarrow \ell\nu)Z(\rightarrow jj)\gamma$  by CMS collaboration at the LHC [19]. These are  $-1.2 \times 10^{-5} \text{ GeV}^{-2} < \frac{k_0}{\Lambda^2} < 1 \times 10^{-5} \text{ GeV}^{-2}$  and  $-1.8 \times 10^{-5} \text{ GeV}^{-2} < \frac{k_c}{\Lambda^2} < 1.7 \times 10^{-5} \text{ GeV}^{-2}$  at 95% C. L..

The LHC which is the current most powerful particle collider, is able to carry out proton-proton collisions at center of mass energy of 14 TeV. It may generate large massive particles and allow us to reveal new physics effects beyond the SM. However, the analysis of the data collected at the LHC is quite difficult due to backgrounds arising from strong interactions. The linear  $e^-e^+$  colliders generally provide clean environment with reference to hadron colliders and they can be used to determine new physics effects with high precision measurements. The Compact Linear Collider (CLIC) is one of the most popular linear colliders, planned to realize  $e^-e^+$  collisions in three energy stages of 0.5, 1.5, and 3 TeV [20]. The CLIC's first energy stage will provide an opportunity the achievement of high precision measurements of various observables of the SM gauge bosons, top quark and Higgs boson. Second energy stage will allow the detection of theories that lie beyond the SM. Moreover, Higgs boson

properties such as the Higgs self-coupling and rare Higgs decay modes will be investigated in this stage [21]. CLIC operating at an energy of 3 TeV reaches a higher effective center-of-mass energy than the LHC for elementary particle collisions [22]. Therefore, this energy stage can be discovered which is unreachable by the LHC. This enables the determination of new particles and the testing of various models as supersymmetry, extra dimensions, and so forth. Besides, the linear colliders have  $e\gamma$  and  $\gamma\gamma$  modes to probe the new physics beyond the SM. High energy real photons in the  $e\gamma$  and  $\gamma\gamma$  processes can be produced by converting the original  $e^-$  or  $e^+$  beam into a photon beam through the Compton back-scattering technique [23, 24]. In addition,  $e\gamma^*$ ,  $\gamma\gamma^*$  and  $\gamma^*\gamma^*$  collisions coming from quasireal photons at the linear colliders also are examined.  $e\gamma^*$  collision is the interaction of an incoming lepton beam and a quasireal  $\gamma^*$  photon associated with the other beam particle;  $\gamma\gamma^*$  collision is the interaction of a real photon and a quasireal photon; and  $\gamma^*\gamma^*$  collision is the interaction between quasireal photons. The photons in these processes uses a Weizsacker-Williams approach, known as the Equivalent Photon Approximation (EPA). In the framework of EPA, the virtuality of the quasireal  $\gamma^*$  photons is very low and they are assumed to be almost real. In EPA, these photons carry a small transverse momentum. Hence, they deviate at very small angles from the incoming lepton beam path. Moreover,  $e\gamma^*$  and  $\gamma^*\gamma^*$  processes are more realistic than  $e\gamma$  and  $\gamma\gamma$  processes since they naturally occur spontaneously from the  $e^-e^+$  process itself. In the literature, photon-induced reactions through the EPA have been extensively studied at the LEP, Tevatron, and LHC [25–51].

## II. CROSS SECTIONS AND NUMERICAL ANALYSIS

In this work, we have applied the  $WWZ\gamma$  vertex into the simulation program, the COM-PHEP, in order to examine numerical calculations [52]. The total cross sections of the process  $e^+e^- \rightarrow W^-W^+\gamma$  are presented in Figs. 1-4 as functions of anomalous  $\frac{k_0}{\Lambda^2}$ ,  $\frac{k_c}{\Lambda^2}$  and  $\frac{a_n}{\Lambda^2}$  couplings with  $\sqrt{s} = 0.5, 1.5$  and 3 TeV. In Figs. 1-4, we consider that only one of the anomalous quartic gauge coupling parameters is non zero at any given time, while the other one coupling is fixed to zero. We can see from Figs. 1-3 that the value of the anomalous cross section including  $\frac{k_0}{\Lambda^2}$  is larger than the value of  $\frac{k_c}{\Lambda^2}$  coupling. Hence, the limits on  $\frac{k_0}{\Lambda^2}$  coupling are expected to be more sensitive according to the limits on  $\frac{k_c}{\Lambda^2}$  coupling. Similarly, the total cross sections of the process  $e^+e^- \rightarrow e^+\gamma^*e^- \rightarrow e^+W^-Z\nu_e$  are presented in Figs.

5-8 as functions of anomalous  $\frac{k_0}{\Lambda^2}$ ,  $\frac{k_c}{\Lambda^2}$  and  $\frac{a_n}{\Lambda^2}$  couplings with  $\sqrt{s} = 0.5, 1.5$  and 3 TeV.

In the course of statistical analysis, the limits of anomalous  $\frac{k_0}{\Lambda^2}$ ,  $\frac{k_c}{\Lambda^2}$  and  $\frac{a_n}{\Lambda^2}$  couplings at 95% C. L. is obtained by using  $\chi^2$  test since the number of SM background events of the examined processes is greater than 10. The  $\chi^2$  function is defined as follows

$$\chi^2 = \left( \frac{\sigma_{SM} - \sigma_{NP}}{\sigma_{SM} \delta_{stat}} \right)^2 \quad (8)$$

where  $\sigma_{NP}$  is the total cross section in the existence of anomalous gauge couplings,  $\delta_{stat} = \frac{1}{\sqrt{N}}$  is the statistical error:  $N$  is the number of events. The number of expected events of the process  $e^+e^- \rightarrow W^-W^+\gamma$  is obtained as the signal  $N = L_{int} \times \sigma_{SM} \times BR(W \rightarrow \ell\nu_\ell) \times BR(W \rightarrow q\bar{q}')$  where  $L_{int}$  is the integrated luminosity,  $\sigma_{SM}$  is the SM cross section and  $\ell = e^-$  or  $\mu^-$ . Similarly, the number of expected events of the process  $e^+e^- \rightarrow e^+\gamma^*e^- \rightarrow e^+W^-Z\nu_e$  is calculated as  $N = L_{int} \times \sigma_{SM} \times BR(W \rightarrow \ell\nu_\ell) \times BR(Z \rightarrow q\bar{q})$ . In addition, we impose the acceptance cuts on the pseudorapidity  $|\eta^\gamma| < 2.5$  and the transverse momentum  $p_T^\gamma > 20$  GeV for photon in the process  $e^+e^- \rightarrow W^-W^+\gamma$ . After applying these cuts, the SM background cross sections for the process  $e^+e^- \rightarrow W^-W^+\gamma$  are calculated as  $1.65 \times 10^{-1}$  pb for  $\sqrt{s} = 0.5$  TeV,  $6.00 \times 10^{-2}$  pb for  $\sqrt{s} = 1.5$  TeV, and  $2.63 \times 10^{-2}$  pb for  $\sqrt{s} = 3$  TeV. However, we estimate as  $3.58 \times 10^{-3}$  pb for  $\sqrt{s} = 0.5$  TeV,  $5.92 \times 10^{-2}$  pb for  $\sqrt{s} = 1.5$  TeV, and  $1.61 \times 10^{-1}$  pb for  $\sqrt{s} = 3$  TeV for the process  $e^+e^- \rightarrow e^+\gamma^*e^- \rightarrow e^+W^-Ze^-$ .

The one-dimensional limits on anomalous couplings  $\frac{k_0}{\Lambda^2}$ ,  $\frac{k_c}{\Lambda^2}$  and  $\frac{a_n}{\Lambda^2}$  at 95% C.L. sensitivity at various integrated luminosities and center-of-mass energies are given in Tables I-II. As can be seen in Table I, the best limits obtained on  $\frac{a_n}{\Lambda^2}$  for the process  $e^+e^- \rightarrow W^-W^+\gamma$  is five orders of magnitude more restrictive than those obtained from the LEP [16] while the limits on  $\frac{k_0}{\Lambda^2}$ ,  $\frac{k_c}{\Lambda^2}$  are approximately an order of magnitude more restrictive than those obtained from the LHC [19]. An important advantage of the examined  $e^+e^- \rightarrow e^+\gamma^*e^- \rightarrow e^+W^-Z\nu_e$  process is that it isolates the anomalous  $WWZ\gamma$  couplings, and therefore it enables to examine  $WWZ\gamma$  couplings independently from  $WW\gamma\gamma$  couplings. We show in Table II that the best limits on the anomalous coupling  $\frac{a_n}{\Lambda^2}$  through the process  $e^+e^- \rightarrow e^+\gamma^*e^- \rightarrow e^+W^-Z\nu_e$  are calculated as  $[-1.17; 1.17] \times 10^{-6}$  GeV $^{-2}$  which are more stringent than LEP's results by almost five orders of magnitude. The limits on the anomalous couplings  $\frac{k_0}{\Lambda^2}$  and  $\frac{k_c}{\Lambda^2}$  are obtained as  $[-6.66; 5.31] \times 10^{-6}$  GeV $^{-2}$  and  $[-8.47; 8.75] \times 10^{-6}$  GeV $^{-2}$  which can improve the sensitivities up to two times for  $\frac{k_0}{\Lambda^2}$  and  $\frac{k_c}{\Lambda^2}$  with respect to LHC's results. In addition, we

compare our limits with phenomenological studies on the anomalous coupling  $\frac{a_n}{\Lambda^2}$ . Our limits are 24 times more restrictive than the best limits obtained with the integrated luminosity of  $100 \text{ fb}^{-1}$  corresponding to  $W^\pm Z\gamma$  production at the 14 TeV LHC [15]. This result is almost of the same order with our result obtained through the processes  $e^+e^- \rightarrow W^-W^+\gamma$  at the CLIC with  $L_{int} = 10 \text{ fb}^{-1}$  and  $\sqrt{s} = 1.5 \text{ TeV}$ . However, Ref. [13] have considered incoming beam polarizations and also the final state polarizations of the gauge bosons in the cross-section calculations to improve the bounds on anomalous  $\frac{a_n}{\Lambda^2}$  coupling. We can see that the limits expected to be obtained for the future  $\gamma\gamma$  colliders with  $L_{int} = 500 \text{ fb}^{-1}$  and  $\sqrt{s} = 1.5 \text{ TeV}$  are 5 times worse than the our best limits when compared to the unpolarized case .

We show 95% C.L. contours in the  $\frac{k_0}{\Lambda^2}-\frac{k_c}{\Lambda^2}$  plane for the  $e^+e^- \rightarrow W^-W^+\gamma$  process in Figs. 9-11 for various integrated luminosity at  $\sqrt{s} = 0.5, 1$  and  $3 \text{ TeV}$ , respectively. Similarly, the same contours for the process  $e^+e^- \rightarrow e^+\gamma^*e^- \rightarrow e^+W^-Z\nu_e$  are depicted in Figs. 12-14. As we can see from Fig. 11, the best limits on anomalous couplings  $\frac{k_0}{\Lambda^2}$  and  $\frac{k_c}{\Lambda^2}$  are  $[-0.33; 0.37] \times 10^{-5} \text{ GeV}^{-2}$  and  $[-0.68; 0.53] \times 10^{-5} \text{ GeV}^{-2}$ , respectively at  $\sqrt{s} = 3 \text{ TeV}$  for  $L_{int} = 590 \text{ fb}^{-1}$ . According to Fig. 14, the attainable limits on  $\frac{k_0}{\Lambda^2}$  and  $\frac{k_c}{\Lambda^2}$  are  $[-0.79; 0.63] \times 10^{-5} \text{ GeV}^{-2}$  and  $[-0.98; 1.08] \times 10^{-5} \text{ GeV}^{-2}$ , respectively.

### III. CONCLUSIONS

The CLIC is an proposed collider with energies on the TeV scale and extremely high luminosity. Particularly, operating with it's high energy and luminosity is extremely important in order to investigate genuie anomalous  $WWZ\gamma$  quartic gauge couplings that are described by dimension 6 effective Lagrangians. Since energy dependences of the anomalous couplings are very high, the anomalous cross sections containing these couplings would have a higher momentum dependence than the SM cross section. We can easily understand that the contribution to the cross section of anomalous quartic couplings rapidly increases when the center-of-mass energy increases. Moreover, the genuie anomalous couplings can obtain higher sensitivity via analyzed reactions in the linear colliders due to very clean experimental conditions and being free from QCD backgrounds with respect to LHC. For these reasons, we have examined the anomalous  $WWZ\gamma$  couplings CP-violating and CP-conserving two different effective Lagrangians through the processes  $e^+e^- \rightarrow W^-W^+\gamma$  and

$e^+e^- \rightarrow e^+\gamma^*e^- \rightarrow e^+W^-Z\nu_e$  at the CLIC.

---

- [1] S. Chatrchyan *et al.*, CMS Collaboration, Phys. Lett. B 716, 30 (2012).
- [2] G. Aad *et al.* ATLAS Collaboration, Phys. Lett. B 716, 1 (2012).
- [3] O. J. P. Eboli, M. C. Gonzalez-Garcia and S. F. Novaes, Nucl. Phys. B411, 381 (1994).
- [4] G. Belanger, F. Boudjema, Y. Kurihara, D. Perret-Gallix, A. Semenov, Eur. Phys. J. C 13 283-293(2000).
- [5] G. Abu Leil and W. J. Stirling, J. Phys. G21, 517 (1995).
- [6] G. Belanger *et al.*, Eur. Phys. J. C13, 283 (2000).
- [7] W. J. Stirling and A. Werthenbach, Eur. Phys. J. C14, 103 (2000).
- [8] A. Denner *et al.*, Eur. Phys. J. C20, 201 (2001).
- [9] G. Montagna *et al.*, Phys. Lett. B515, 197 (2001).
- [10] M. Beyer *et al.*, Eur. Phys. J. C48, 353 (2006).
- [11] I. Sahin, J. Phys. G: Nucl. Part. Phys. 35 035006 (2008).
- [12] O. J. P. Eboli, M. B. Magro, P. G. Mercadante and S. F. Novaes, Phys. Rev. D52, 15 (1995).
- [13] I. Sahin, J. Phys. G: Nucl. Part. Phys. 36 075007 (2009).
- [14] O. J. P. Eboli, M.C. Gonzalez-Garcia, S. M. Lietti, Phys. Rev. D 69 095005 (2004).
- [15] Ke Ye, Daneng Yang, Qiang Li, Phys.Rev. D 88 1 015023 (2013).
- [16] P. Achard *et al.*, L3 Collaboration, Phys. Lett. B527, 29 (2002).
- [17] J. Abdallah *et al.*, DELPHI Collaboration, Eur. Phys. J. C31, 139 (2003).
- [18] G. Abbiendi *et al.*, OPAL Collaboration, Phys. Lett. B580, 17 (2004).
- [19] S. Chatrchyan *et al.*, CMS Collaboration, arXiv:1404.4619 [hep-ex].
- [20] D. Dannheim *et al.*, CLIC  $e^+e^-$  Linear Collider Studies, arXiv:1305.5766v1.
- [21] D. Dannheim *et al.*, CLIC  $e^+e^-$  Linear Collider Studies, arXiv:1208.1402.
- [22] L. Linssen, A. Miyamoto, M. Stanitzki and H. Weerts, CERN-2012-003 ; ANL-HEP-TR-12-01 ; DESY-12-008 ; KEK-Report-2011-7.
- [23] I. F. Ginzburg, G. L. Kotkin, V. G. Serbo and V. I. Telnov, Nucl. Instr. and Meth. 205 47 (1983).
- [24] I. F. Ginzburg, G. L. Kotkin, S. L. Panfil, V. G. Serbo and V. I. Telnov, Nucl. Instr. and Meth. 219 5 (1984).



- [25] J. Abdallah *et al.*, DELPHI Collaboration, Eur. Phys. J. C 35 159 (2004).
- [26] A. Abulencia *et al.*, CDF Collaboration, Phys. Rev. Lett. 98 112001 (2007).
- [27] T. Aaltonen *et al.*, CDF Collaboration, Phys. Rev. Lett. 102 222002 (2009).
- [28] T. Aaltonen *et al.*, CDF Collaboration, Phys. Rev. Lett. 102 242001 (2009).
- [29] S. Chatrchyan *et al.*, CMS Collaboration, JHEP 1201 052 (2012).
- [30] S. Chatrchyan *et al.*, CMS Collaboration, JHEP 1211 080 (2012).
- [31] S. Atag and A. Billur, JHEP 11 060 (2010).
- [32] S. Atag, S. C. İnan and İ. Şahin, Phys. Rev. D 80 075009 (2009).
- [33] İ. Şahin and S. C. İnan, JHEP 09 069 (2009).
- [34] S. C. İnan, Phys. Rev. D 81 115002 (2010).
- [35] İ. Şahin and M. Köksal, JHEP 11 100 (2011).
- [36] M. Köksal and S. C. İnan, arXiv:1305.7096.
- [37] M. Köksal and S. C. İnan, AHEP Volume 2014, Article ID 315826, 8 pages (2014).
- [38] A. A. Billur and M. Köksal, Phys. Rev. D 89 037301 (2014).
- [39] A. A. Billur and M. Köksal, arXiv:1311.5326.
- [40] A. Senol, Phys. Rev. D 87 7 073003 (2013).
- [41] A. Senol, arXiv:1311.1370.
- [42] İ. Şahin *et al.*, Phys.Rev. D 88 095016 (2013).
- [43] S. C. İnan and A. Billur, Phys. Rev. D 84 095002 (2011).
- [44] İ. Şahin, Phys. Rev. D 85 033002 (2012).
- [45] İ. Şahin and B. Şahin, Phys. Rev. D 86 115001 (2012).
- [46] B. Şahin and A. A. Billur, Phys. Rev. D 86 074026 (2012).
- [47] A. A. Billur, Europhys. Lett. 101 21001 (2013).
- [48] M. Tasevsky, Nucl. Phys. Proc. Suppl. 179-180 187-195 (2008).
- [49] M. Tasevsky, arXiv:0910.5205.
- [50] H. Sun, arXiv:1402.1817.
- [51] H. Sun and Chong-Xing Yue, Eur.Phys.J. C 74 2823 (2014).
- [52] A. Pukhov *et al.*, Report No. INP MSU 98-41/542; arXiv:hep-ph/9908288; arXiv:hep-ph/0412191.

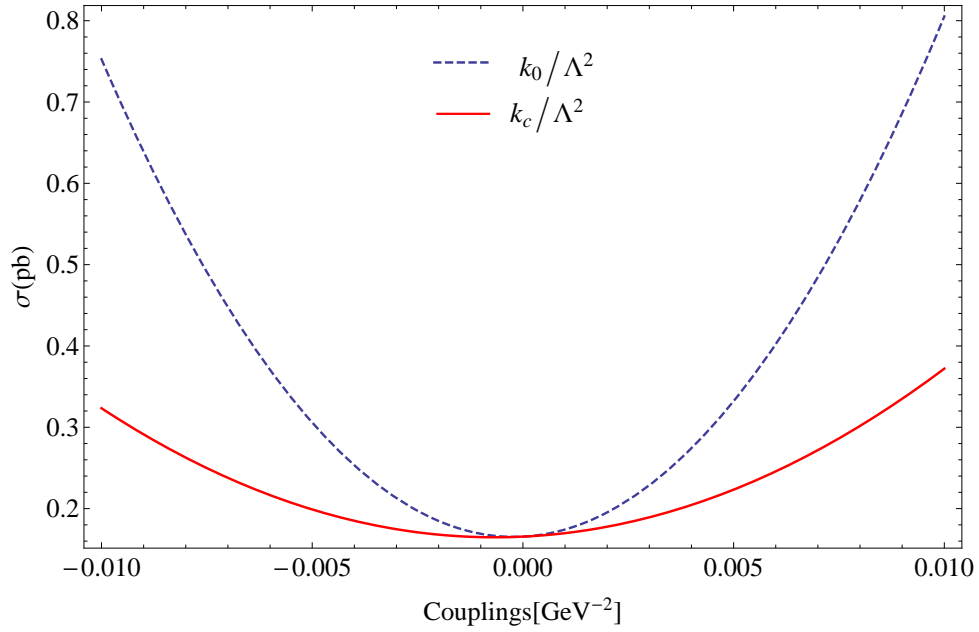


FIG. 1: The total cross sections as function of anomalous  $\frac{k_0}{\Lambda^2}$  and  $\frac{k_c}{\Lambda^2}$  couplings for the  $e^+e^- \rightarrow W^-W^+\gamma$  at the CLIC with  $\sqrt{s} = 0.5$  TeV.

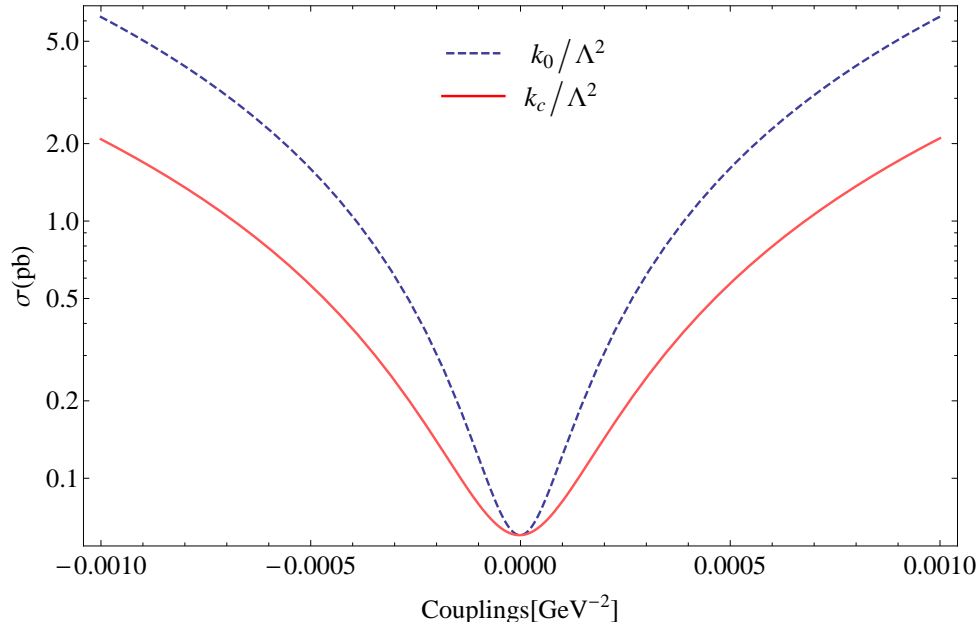


FIG. 2: The same as Fig. 1 but for  $\sqrt{s} = 1.5$  TeV.

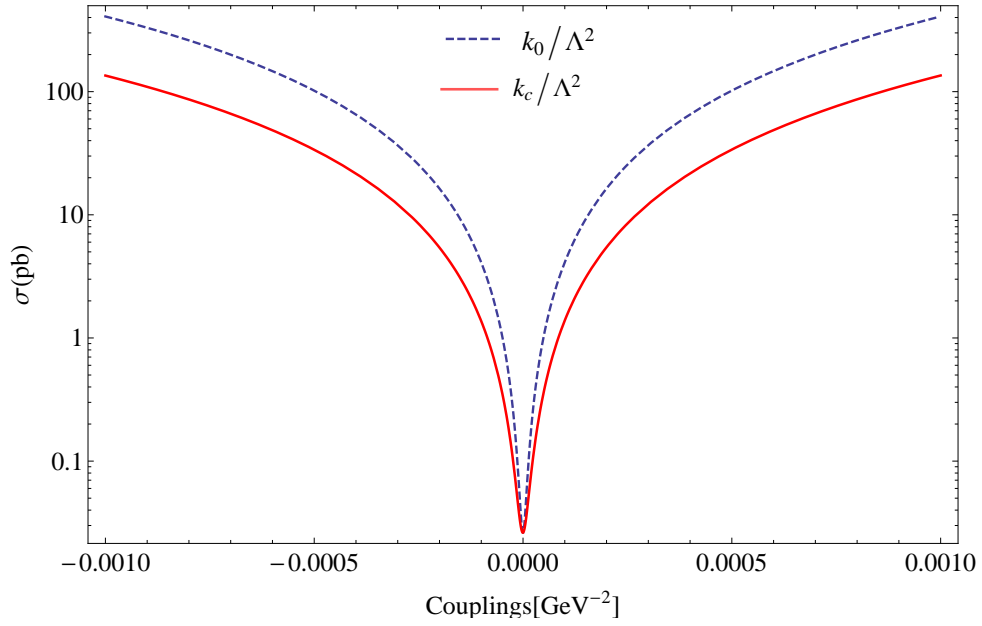


FIG. 3: The same as Fig. 1 but for  $\sqrt{s} = 3$  TeV.

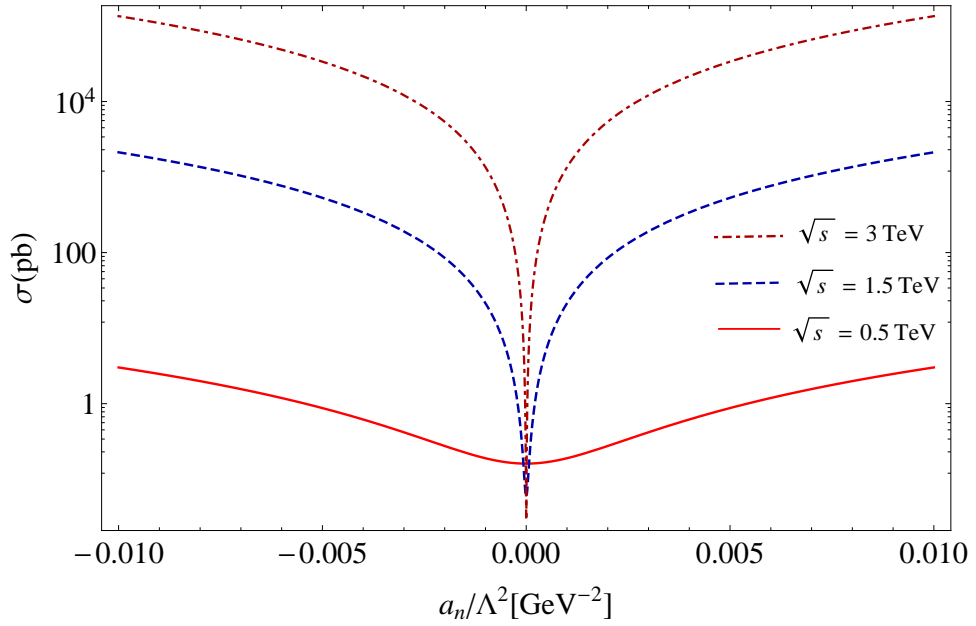


FIG. 4: The total cross sections as function of anomalous  $\frac{a_n}{\Lambda^2}$  coupling for the process  $e^+e^- \rightarrow W^-W^+\gamma$  at the CLIC with  $\sqrt{s} = 0.5, 1.5$  and 3 TeV.

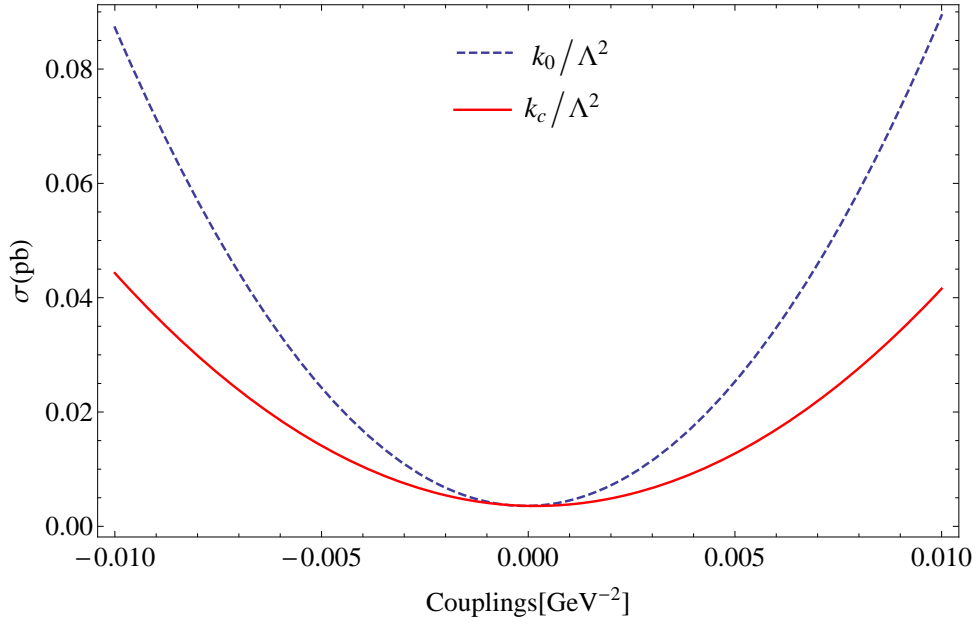


FIG. 5: The total cross sections as function of anomalous  $\frac{k_0}{\Lambda^2}$  and  $\frac{k_c}{\Lambda^2}$  couplings for the process  $e^+e^- \rightarrow e^+\gamma^*e^- \rightarrow e^+W^-Z\nu_e$  at the CLIC with  $\sqrt{s} = 0.5$  TeV.

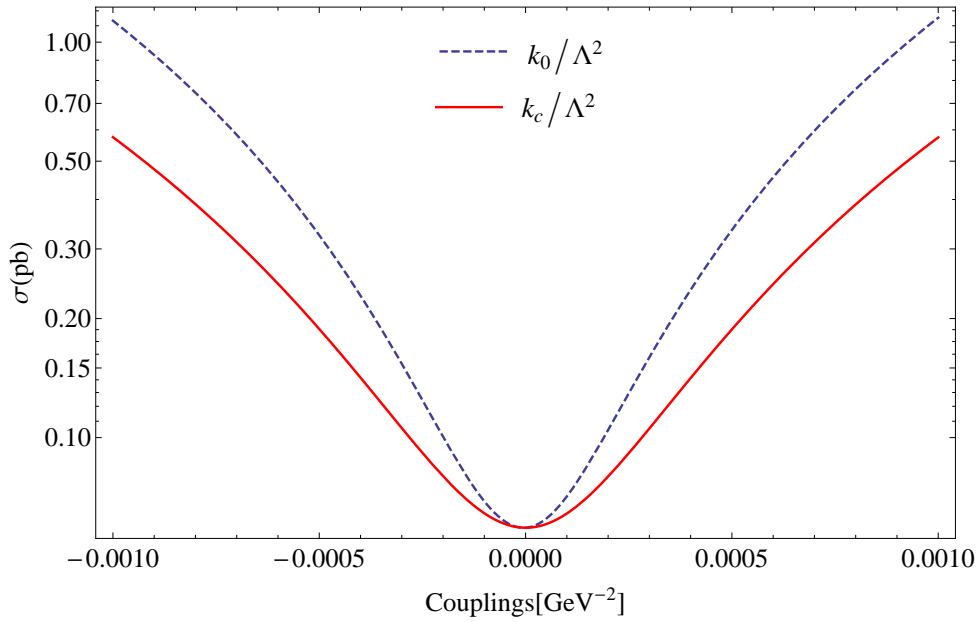


FIG. 6: The same as Fig. 5 but for  $\sqrt{s} = 1.5$  TeV.

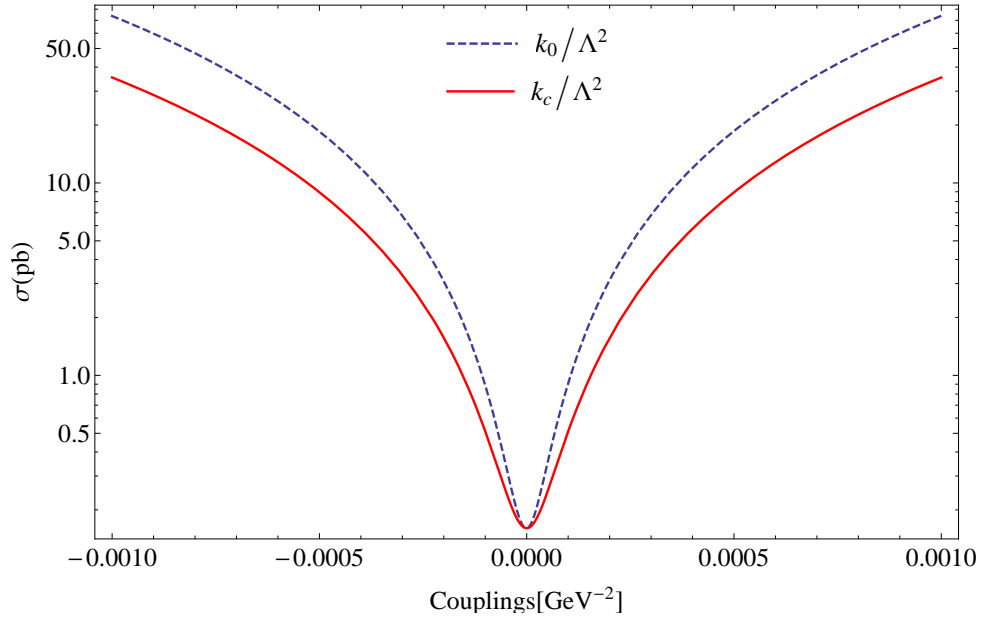


FIG. 7: The same as Fig. 5 but for  $\sqrt{s} = 3$  TeV.

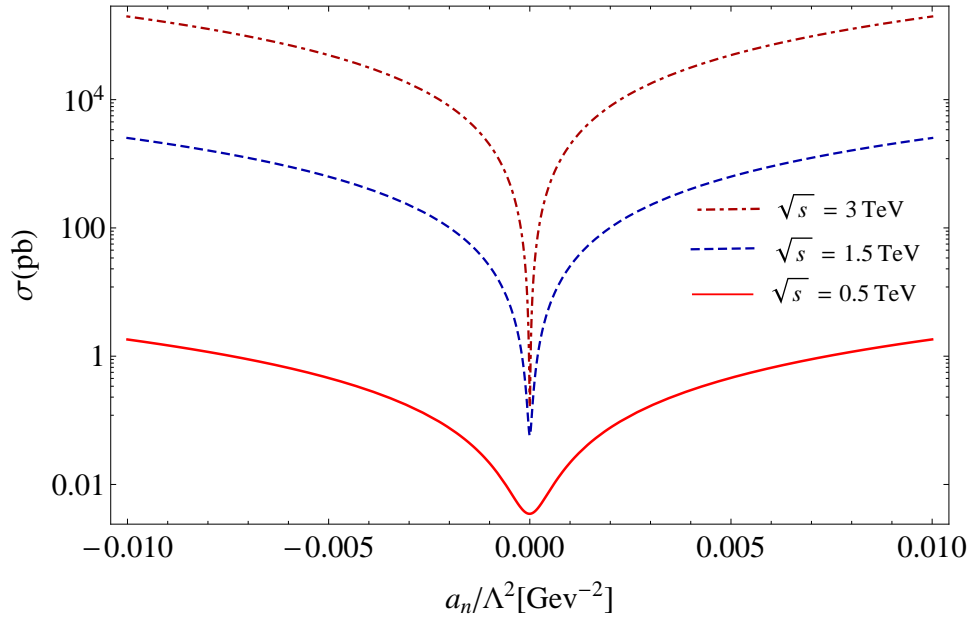


FIG. 8: The total cross sections as function of anomalous  $\frac{a_n}{\Lambda^2}$  coupling for the process  $e^+e^- \rightarrow e^+\gamma^*e^- \rightarrow e^+W^-Z\nu_e$  at the CLIC with  $\sqrt{s} = 0.5, 1.5$  and 3 TeV.

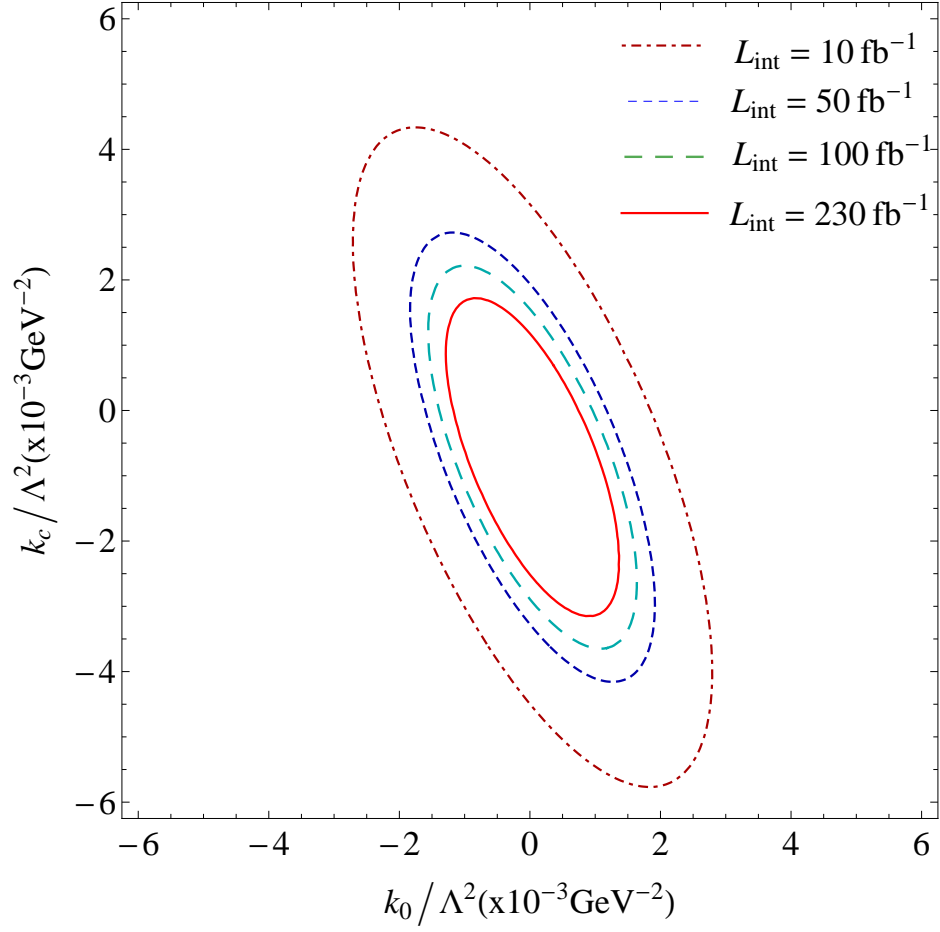


FIG. 9: 95% C.L. contours for anomalous  $\frac{k_0}{\Lambda^2}$  and  $\frac{k_c}{\Lambda^2}$  couplings for the process  $e^+e^- \rightarrow W^-W^+\gamma$  at the CLIC with  $\sqrt{s} = 0.5$  TeV.

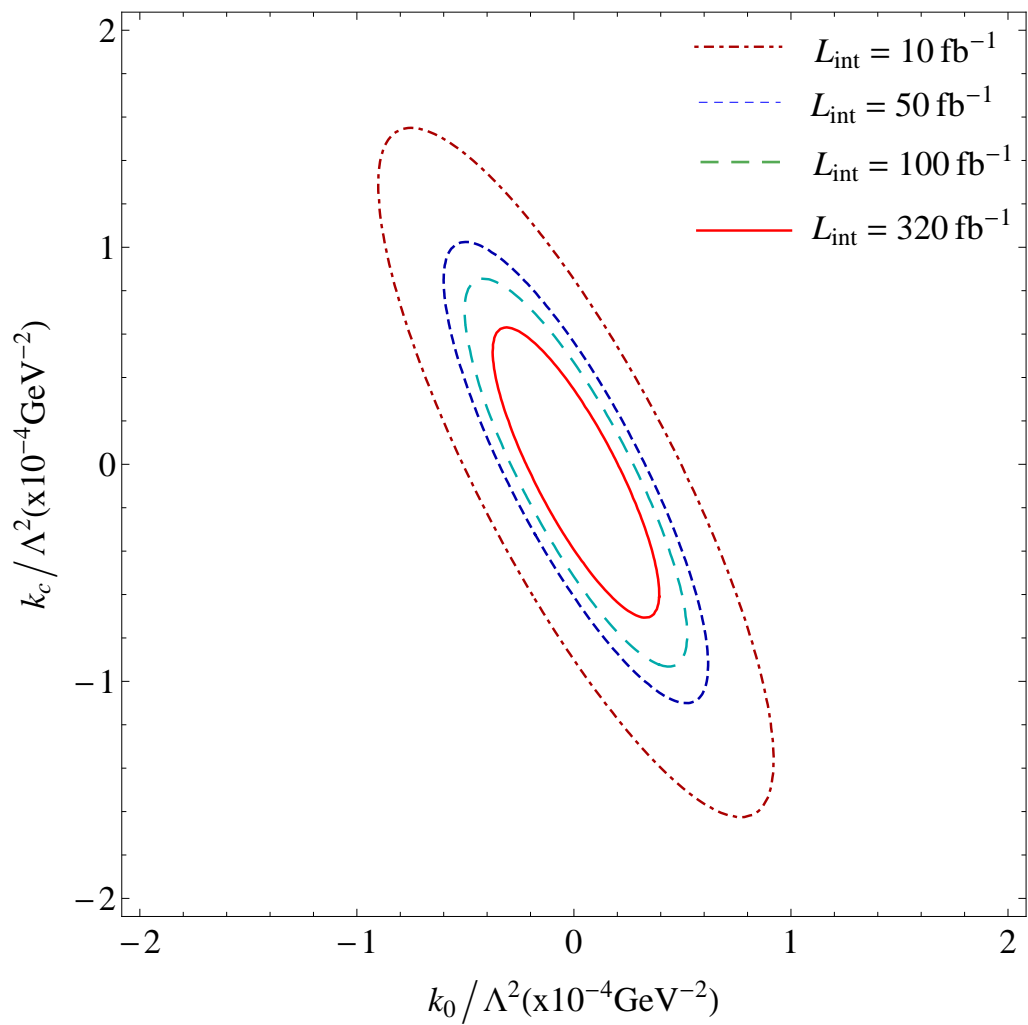


FIG. 10: The same as Fig. 9 but for  $\sqrt{s} = 1.5$  TeV.

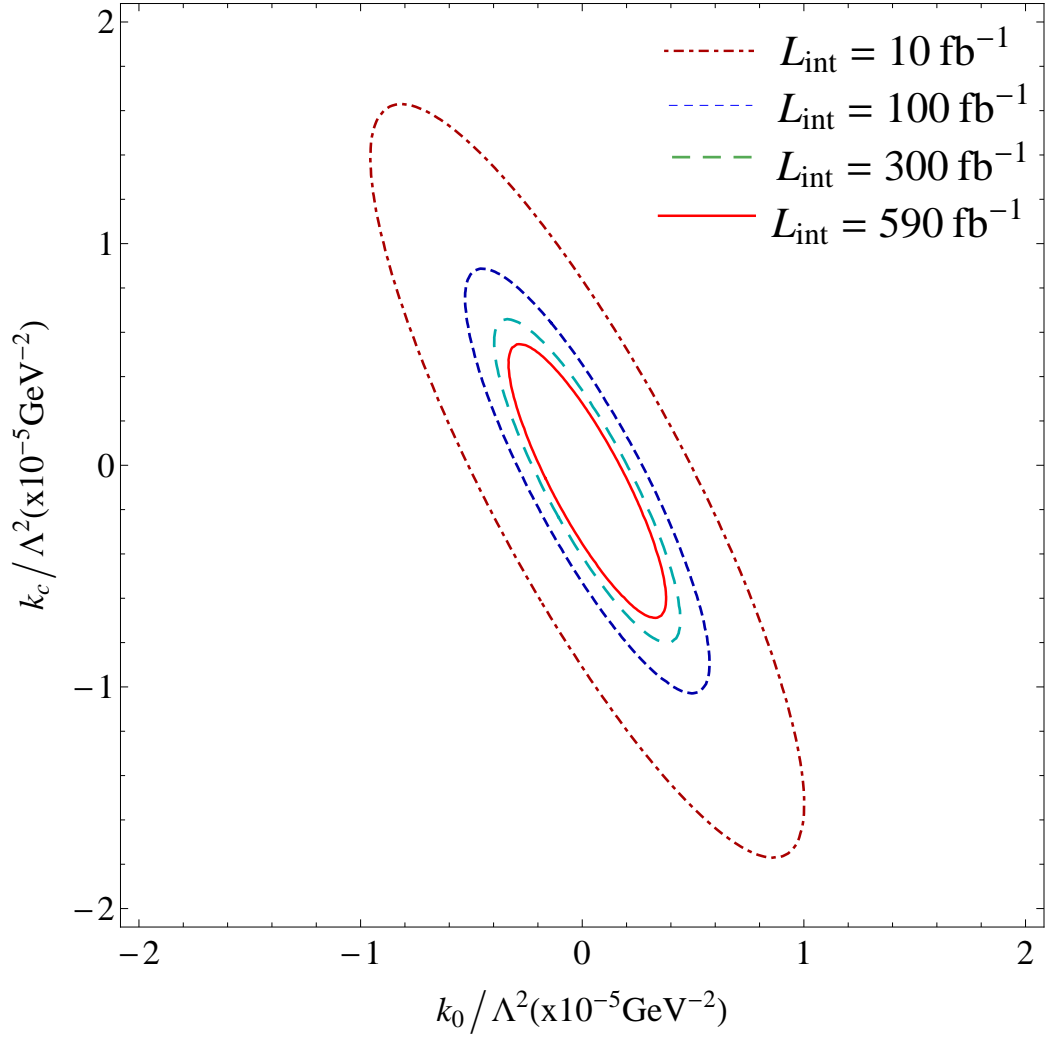


FIG. 11: The same as Fig. 9 but for  $\sqrt{s} = 3 \text{ TeV}$ .



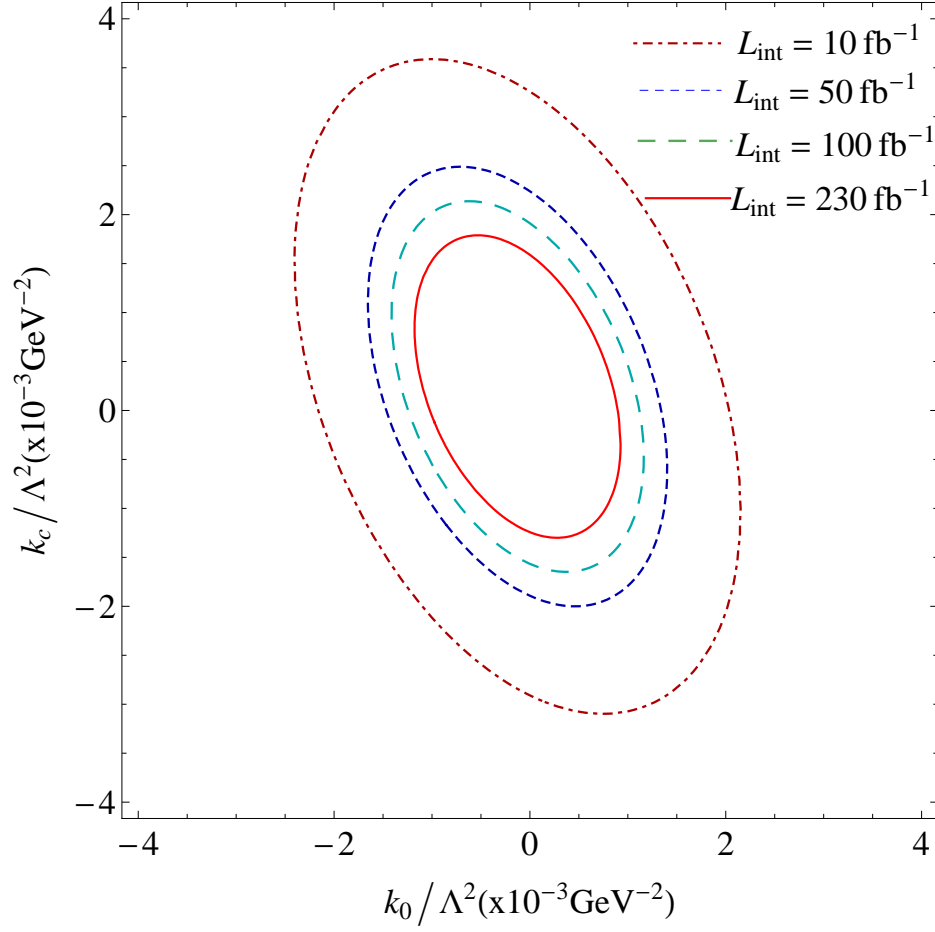


FIG. 12: 95% C.L. contours for anomalous  $\frac{k_0}{\Lambda^2}$  and  $\frac{k_c}{\Lambda^2}$  couplings for the process  $e^+e^- \rightarrow e^+\gamma^*e^- \rightarrow e^+W^-Z\nu_e$  at the CLIC with  $\sqrt{s} = 0.5$  TeV.

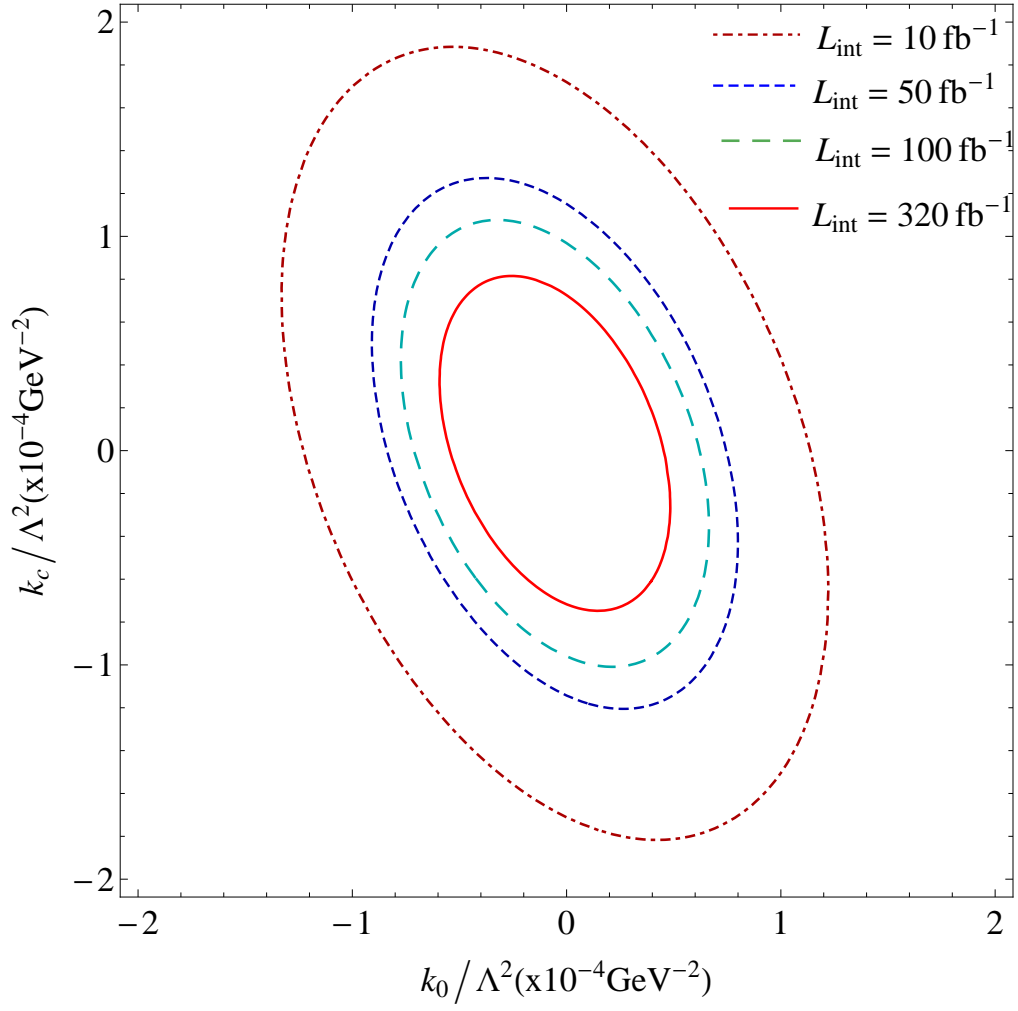


FIG. 13: The same as Fig. 12 but for  $\sqrt{s} = 1.5$  TeV.

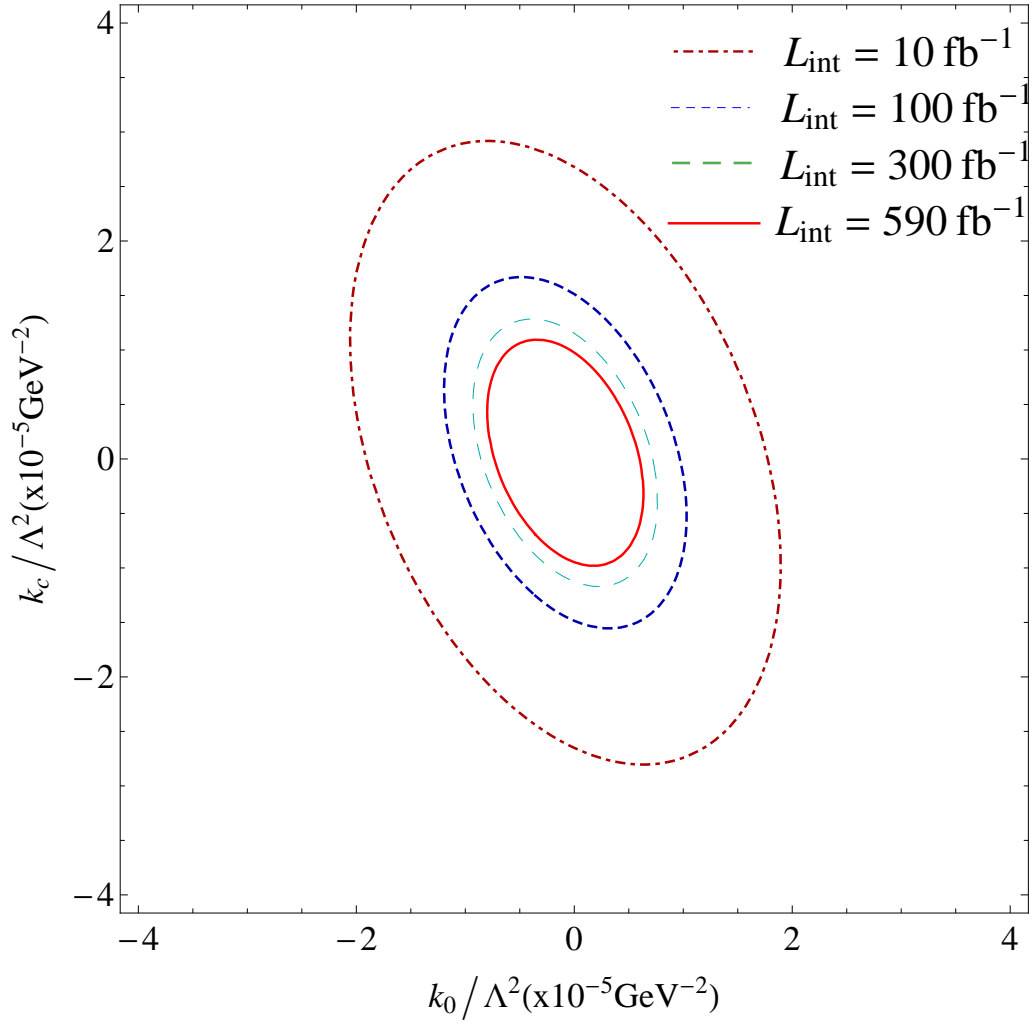


FIG. 14: The same as Fig. 12 but for  $\sqrt{s} = 3 \text{ TeV}$ .

TABLE I: 95% C.L. sensitivity bounds of the  $\frac{k_0}{\Lambda^2}$ ,  $\frac{k_c}{\Lambda^2}$  and  $\frac{a_n}{\Lambda^2}$  couplings through the process  $e^+e^- \rightarrow W^-W^+\gamma$  at the CLIC with  $\sqrt{s} = 0.5, 1.5$  and 3 TeV.

| $\sqrt{s}$ (TeV) | $L_{int}(\text{fb}^{-1})$ | $\frac{k_0}{\Lambda^2}(\text{GeV}^{-2})$ | $\frac{k_c}{\Lambda^2}(\text{GeV}^{-2})$ | $\frac{a_n}{\Lambda^2}(\text{GeV}^{-2})$ |
|------------------|---------------------------|--|--|--|
| 0.5              | 10                        | $[-2.06; 1.63] \times 10^{-3}$           | $[-4.11; 2.77] \times 10^{-3}$           | $[-8.47; 8.45] \times 10^{-4}$           |
| 0.5              | 50                        | $[-1.46; 1.03] \times 10^{-3}$           | $[-3.02; 1.68] \times 10^{-3}$           | $[-5.67; 5.65] \times 10^{-4}$           |
| 0.5              | 100                       | $[-1.27; 0.84] \times 10^{-3}$           | $[-2.68; 1.34] \times 10^{-3}$           | $[-4.77; 4.75] \times 10^{-4}$           |
| 0.5              | 230                       | $[-1.08; 0.65] \times 10^{-3}$           | $[-2.35; 1.01] \times 10^{-3}$           | $[-3.88; 3.85] \times 10^{-4}$           |
| 1.5              | 10                        | $[-4.59; 4.41] \times 10^{-5}$           | $[-8.09; 7.60] \times 10^{-5}$           | $[-2.59; 2.57] \times 10^{-5}$           |
| 1.5              | 50                        | $[-3.10; 2.92] \times 10^{-5}$           | $[-5.49; 5.01] \times 10^{-5}$           | $[-1.85; 1.83] \times 10^{-5}$           |
| 1.5              | 100                       | $[-2.62; 2.46] \times 10^{-5}$           | $[-4.66; 4.17] \times 10^{-5}$           | $[-1.63; 1.61] \times 10^{-5}$           |
| 1.5              | 320                       | $[-1.98; 1.81] \times 10^{-5}$           | $[-3.55; 3.06] \times 10^{-5}$           | $[-1.35; 1.33] \times 10^{-5}$           |
| 3                | 10                        | $[-4.62; 4.38] \times 10^{-6}$           | $[-8.19; 7.46] \times 10^{-6}$           | $[-2.46; 2.46] \times 10^{-6}$           |
| 3                | 100                       | $[-2.66; 2.41] \times 10^{-6}$           | $[-4.78; 4.04] \times 10^{-6}$           | $[-1.38; 1.38] \times 10^{-6}$           |
| 3                | 300                       | $[-2.05; 1.80] \times 10^{-6}$           | $[-3.73; 2.99] \times 10^{-6}$           | $[-1.05; 1.05] \times 10^{-6}$           |
| 3                | 590                       | $[-1.75; 1.50] \times 10^{-6}$           | $[-3.21; 2.47] \times 10^{-6}$           | $[-9.13; 9.09] \times 10^{-7}$           |

TABLE II: 95% C.L. sensitivity bounds of the  $\frac{k_0}{\Lambda^2}$ ,  $\frac{k_c}{\Lambda^2}$  and  $\frac{a_n}{\Lambda^2}$  couplings through the processes  $e^+e^- \rightarrow e^+\gamma^*e^- \rightarrow e^+W^-\gamma\nu_e$  at the CLIC with  $\sqrt{s} = 0.5, 1.5$  and 3 TeV.

| $\sqrt{s}$ (TeV) | $L_{int}(\text{fb}^{-1})$ | $\frac{k_0}{\Lambda^2}(\text{GeV}^{-2})$ | $\frac{k_c}{\Lambda^2}(\text{GeV}^{-2})$ | $\frac{a_n}{\Lambda^2}(\text{GeV}^{-2})$ |
|------------------|---------------------------|--|--|--|
| 0.5              | 10                        | $[-1.94; 1.82] \times 10^{-3}$           | $[-2.59; 2.93] \times 10^{-3}$           | $[-4.08; 3.96] \times 10^{-4}$           |
| 0.5              | 50                        | $[-1.32; 1.19] \times 10^{-3}$           | $[-1.67; 2.02] \times 10^{-3}$           | $[-2.75; 2.63] \times 10^{-4}$           |
| 0.5              | 100                       | $[-1.12; 1.00] \times 10^{-3}$           | $[-1.38; 1.73] \times 10^{-3}$           | $[-2.33; 2.20] \times 10^{-4}$           |
| 0.5              | 230                       | $[-9.22; 7.97] \times 10^{-4}$           | $[-1.10; 1.14] \times 10^{-3}$           | $[-1.90; 1.78] \times 10^{-4}$           |
| 1.5              | 10                        | $[-1.11; 1.01] \times 10^{-4}$           | $[-1.53; 1.54] \times 10^{-4}$           | $[-2.19; 2.17] \times 10^{-5}$           |
| 1.5              | 50                        | $[-7.55; 6.64] \times 10^{-5}$           | $[-1.02; 1.03] \times 10^{-4}$           | $[-1.47; 1.45] \times 10^{-5}$           |
| 1.5              | 100                       | $[-6.43; 5.51] \times 10^{-5}$           | $[-8.59; 8.68] \times 10^{-5}$           | $[-1.23; 1.22] \times 10^{-5}$           |
| 1.5              | 320                       | $[-4.93; 4.02] \times 10^{-5}$           | $[-6.41; 6.50] \times 10^{-5}$           | $[-9.26; 9.07] \times 10^{-6}$           |
| 3                | 10                        | $[-1.72; 1.58] \times 10^{-5}$           | $[-2.37; 2.40] \times 10^{-5}$           | $[-3.16; 3.16] \times 10^{-6}$           |
| 3                | 100                       | $[-1.01; 0.87] \times 10^{-5}$           | $[-1.33; 1.36] \times 10^{-5}$           | $[-1.78; 1.77] \times 10^{-6}$           |
| 3                | 300                       | $[-7.75; 6.40] \times 10^{-6}$           | $[-1.01; 1.03] \times 10^{-5}$           | $[-1.35; 1.35] \times 10^{-6}$           |
| 3                | 590                       | $[-6.66; 5.31] \times 10^{-6}$           | $[-8.47; 8.75] \times 10^{-6}$           | $[-1.17; 1.17] \times 10^{-6}$           |